

Reactions of Distibines Sb_2R_4 and Dibismuthine Bi_2Et_4 with Trialkyltrienes MR_3

A. Kuczkowski, S. Fahrenholz, S. Schulz,* and M. Nieger

Institut für Anorganische Chemie der Universität Bonn, Gerhard-Domagk-Strasse 1, D-53121 Bonn, Germany

Received April 8, 2004

Distibines Sb_2R_4 react with trimethylgallane and -indane (MMe_3 ; $\text{M} = \text{Ga}, \text{In}$) with formation of heterocycles of the general type $[\text{Me}_2\text{MSbR}'_2]_3$ ($\text{R}' = \text{Me}, \text{M} = \text{Ga}$ (**2**), In (**3**); $\text{R}' = i\text{-Pr}, \text{M} = \text{Ga}$ (**4**)), whereas only decomposition reactions were observed for reactions with trialkylalanes. However, the mononuclear distibine–alane adduct $[\text{Al}(t\text{-Bu})_3][\text{Sb}_2(i\text{-Pr})_4]$ (**1**) with the distibine serving as monodentate ligand could be isolated and structurally characterized. In addition, reactions of the dibismuthine Bi_2Et_4 with $\text{M}(t\text{-Bu})_3$ ($\text{M} = \text{Al}, \text{Ga}$) were investigated, resulting in the formation of the simple Lewis acid–base adducts $\text{Et}_3\text{Bi-M}(t\text{-Bu})_3$ ($\text{M} = \text{Al}$ (**5**), Ga (**6**)). **1–6** were characterized by multinuclear NMR and mass spectroscopy and elemental analysis as well as single-crystal X-ray diffraction.

Introduction

Reactions of Lewis bases ER'_3 ($\text{E} = \text{N}, \text{P}, \text{As}, \text{Sb}, \text{Bi}$) with Lewis acids MR_3 ($\text{M} = \text{B}, \text{Al}, \text{Ga}, \text{In}, \text{Tl}$) have been investigated for almost two centuries.¹ In sharp contrast, reactions of dipenteles of the type $\text{R}'_2\text{E-ER}'_2$, which may serve as both monodentate² and bidentate ligands,³ as was shown in several reactions with transition-metal complexes, and MR_3 have been studied to a far lesser extent. Only two dinuclear diphosphine–borane adducts ($[\text{Me}_4\text{P}_2][\text{BH}_3]_2$, $[\text{Me}_4\text{P}_2][\text{BH}_2\text{Br}]_2$)⁴ have been synthesized and structurally characterized prior to our studies. We became only recently interested in such types of compounds and reported on the synthesis and single-crystal X-ray structures of the first dinuclear distibine⁵ and dibismuthine adducts,⁶ with the dipentele serving as a bidentate ligand. These adducts were found to be fairly stable in their pure forms, whereas they tend to undergo consecutive reactions in solution. The distibine–gallane adducts $[\text{R}_4\text{Sb}_2]$ -

$[\text{Ga}(t\text{-Bu})_3]_2$ ($\text{R} = \text{Me}, \text{Et}$) were found to react at ambient temperature with formation of the heterocyclic stibinogallanes $[t\text{-Bu}_2\text{GaSbMe}_2]_3$ and $[t\text{-Bu}_2\text{GaSbEt}_2]_2$.⁵ This reaction, which has also been observed by Breunig et al. on the reaction of Sb_2Me_4 with $\text{In}(\text{CH}_2\text{SiMe}_3)_3$,⁷ is most likely based on the lability of the Sb–Sb bond toward electrophilic compounds.⁸ Comparable reactions have been previously observed for distibine transition-metal complexes.⁹

Due to our interest in completely alkyl-substituted Ga–Sb and In–Sb heterocycles, which are promising candidates for the deposition of thin films of the corresponding binary antimonides GaSb and InSb by the MOCVD (*metal organic chemical vapor deposition*) process,¹⁰ we investigated the general applicability of this reaction pathway for the synthesis of the desired class of M–Sb heterocycles. In addition, reactions of the dibismuthine Bi_2Et_4 with $\text{M}(t\text{-Bu})_3$ ($\text{M} = \text{Al}, \text{Ga}$) were studied in order to investigate whether this reaction type can also be assigned for the synthesis of M–Bi heterocycles.

Experimental Section

General Considerations. All manipulations were performed in a glovebox under a N_2 atmosphere or by standard Schlenk techniques. $\text{Al}(t\text{-Bu})_3$,¹¹ GaMe_3 ,¹² InMe_3 ,¹³ Sb_2Me_4 ,¹⁴ Sb_2Et_4 ,¹⁵ $\text{Sb}_2(i\text{-Pr})_4$,¹⁶ and Bi_2Et_4 ¹⁷ were prepared according to literature methods. ^1H and $^{13}\text{C}\{^1\text{H}\}$ spectra were recorded using a Bruker AMX 300 spectrometer and are referenced to internal $\text{C}_6\text{D}_5\text{H}$ ($\delta(^1\text{H})$ 7.154, $\delta(^{13}\text{C})$ 128.0). Melting points were measured in sealed capillaries and are not corrected. Mass spectra were recorded on a VG Masslab 12-250 spectrometer

(7) Breunig, H. J.; Stanciu, M.; Rösler, R.; Lork, E. *Z. Anorg. Allg. Chem.* **1998**, *624*, 1965.

(8) Samaan, S. In *Houben Weyl: Methoden der Organischen Chemie*, 4th ed.; Thieme Verlag: Stuttgart, Germany, 1978; Metallorganische Verbindungen des Arsens, Antimons und Bismuts.

(9) Breunig, H. J.; Fichtner, W. *Z. Anorg. Allg. Chem.* **1981**, *477*, 119.

(10) (a) Cowley, A. H.; Jones, R. A.; Nunn, C. M.; Westmoreland, D. L. *Chem. Mater.* **1990**, *2*, 221. (b) Park, H. S.; Schulz, S.; Wessel, H.; Roesky, H. W. *Chem. Vap. Deposition* **1999**, *5*, 179.

* To whom correspondence should be addressed. Phone: +(49)228-73-5326. Fax: +(49)228-73-5327. E-mail: sschulz@uni-bonn.de.

(1) The synthesis of $\text{F}_3\text{B-NH}_3$ was reported by Gay-Lussac almost 200 years ago (Gay-Lussac, J. L.; Thenard, J. L. *Mém. Phys. Chim. Soc. d'Arcueil* **1809**, *2*, 210. Cited in: Jonas, V.; Frenking, G. *Chem. Commun.* **1994**, 1489).

(2) For a recent review see: Breunig, H. J. *Adv. Organomet. Chem.* **2003**, *49*, 95.

(3) (a) Bailey, N. A.; Frisch, P. D.; McCleverty, J. A.; Walker, N. W. J.; Williams, J. J. *J. Chem. Soc., Chem. Commun.* **1975**, 350. (b) Bultitude, J.; Larkworthy, L. F.; Povey, D. C.; Smith, G. W.; Dilworth, J. R.; Leigh, G. J. *J. Chem. Soc., Chem. Commun.* **1986**, 1748. (c) Vogel, S.; Barth, A.; Huttner, G.; Klein, T.; Zsolnai, L.; Kremer, R. *Angew. Chem., Int. Ed. Engl.* **1991**, *30*, 303. (d) Schrock, R. R.; Glassman, T. E.; Vale, M. G.; Kol, M. *J. Am. Chem. Soc.* **1993**, *115*, 1760. (e) Sharma, P.; Rosas, N.; Hernandez, S.; Cabrera, A. *J. Chem. Soc., Chem. Commun.* **1995**, 1325.

(4) (a) Nöth, H. *Z. Naturforsch., B* **1960**, *15*, 327. (b) Burg, A. B.; Wagner, R. I. *J. Am. Chem. Soc.* **1953**, *75*, 3872. (c) Burg, A. B.; Brendel, J. *J. Am. Chem. Soc.* **1958**, *80*, 3198. (d) Burg, A. B. *J. Am. Chem. Soc.* **1961**, *83*, 2226. (e) Carrell, H. L.; Donohue, J. *Acta Crystallogr., Sect. B* **1968**, *24*, 699. (f) Schmidbaur, H.; Wimmer, T.; Grohmann, A.; Steigelmann, O.; Müller, G. *Chem. Ber.* **1989**, *122*, 1607.

(5) Kuczkowski, A.; Schulz, S.; Nieger, M.; Saarenketo, P. *Organometallics* **2001**, *20*, 2000.

(6) Kuczkowski, A.; Schulz, S.; Nieger, M. *Angew. Chem., Int. Ed.* **2001**, *40*, 4222.

in the electron ionization mode at 20 eV. Elemental analyses were performed at the Mikroanalytisches Labor der Universität Bonn.

[*i*-Pr₄Sb₂][Al(*t*-Bu)₃] (1; M_r = 614.19). Pure Al(*t*-Bu)₃ (2 mmol, 0.40 g) and Sb₂(*i*-Pr)₄ (2 mmol, 0.83 g) were combined in the glovebox. The resulting yellow oil was dissolved in pentane (5 mL) and stored at -60 °C, resulting in the formation of light yellow crystals of **1**. Yield: 0.59 g, 0.96 mmol, 48%. Mp: ca. -30 °C. Anal. Found (calcd) for C₄₄H₅₅AlSb₂: C, 46.78 (46.90); H, 9.22 (9.35). ¹H NMR (300 MHz, C₆D₅H, 25 °C): δ 1.17 (s, 27 H, Me₃C/Al), 1.42 (d, ³J_{HH} = 7.3 Hz, 6 H, Me₂CH/Sb), 1.48 (d, ³J_{HH} = 7.3 Hz, 6 H, Me₂CH/Sb), 2.34 (sept, ³J_{HH} = 7.3 Hz, 4 H, Me₂CH/Sb). ¹³C{¹H} NMR (80 MHz, C₆D₅H, 25 °C): δ 14.4 (Me₂CH/Sb), 20.3 (Me₃C/Al), 24.9 (Me₂CH/Sb), 31.4 (Me₃C/Al).

[Me₂GaSbMe₂]₃ (2; M_r = 754.83). A 2 mmol portion of Sb₂Me₄ (0.60 g) was added to a solution of 3.8 mmol of GaMe₃ (0.44 g) dissolved in 40 mL of pentane. The resulting yellow solution was stirred for 5 days at ambient temperature in the absence of light, yielding a colorless solution. The solvent was reduced to 5 mL and the solution stored at -60 °C. After 72 h, **2** was obtained as a colorless powder. Yield: 0.34 g, 0.45 mmol, 68% (based on the distibine). Mp: 92–94 °C dec. Anal. Found (calcd) for C₁₂H₃₆Ga₃Sb₃: C, 18.99 (19.10); H, 4.66 (4.80). ¹H NMR (300 MHz, C₆D₅H, 25 °C): δ 0.19 (s, 6H, Me/Ga), 0.84 (s, 6H, Me/Sb). ¹³C{¹H} NMR (75 MHz, C₆D₆, 25 °C): δ -6.1 (Me/Sb), 1.4 (Me/Ga). EI-MS (*m/z* (%)): 485 (3) [Me₇Sb₂Ga₂]⁺, 304 (100) [Me₃SbGa₂]⁺, 289 (76) [Me₂SbGa₂]⁺, 274 (15) [MeSbGa₂]⁺, 259 (5) [SbGa₂]⁺, 153 (89) [MeGa₂]⁺, 151 (29) [Me₂Sb]⁺, 136 (27) [MeSb]⁺, 84 (5) [MeGa]⁺.

[Me₂InSbMe₂]₃ (3; M_r = 890.12). A 4 mmol portion of InMe₃ (0.64 g) and 2 mmol of Sb₂Me₄ (0.60 g) were dissolved in 30 mL of toluene and stirred for 5 days at ambient temperature in the absence of light. After evaporation of the solvent, the resulting colorless solid was dissolved in 30 mL of hexane. After filtration, a colorless solution was obtained, which was concentrated to 10 mL and stored at -30 °C. After 72 h, **3** was obtained as colorless crystals. Yield: 0.77 g, 0.86 mmol, 43% (based on the distibine). Mp: 64–66 °C dec. Anal. Found (calcd) for C₁₂H₃₆In₃Sb₃: C, 16.56 (16.21); H, 4.24 (4.01). ¹H NMR (300 MHz, C₆D₅H, 25 °C): δ 0.93 (s, 6H, Me/Sb), 0.19 (s, 6H, Me/In). ¹³C{¹H} NMR (75 MHz, C₆D₆, 25 °C): δ -11.2 (Me/Sb), 1.4 (Me/In). EI-MS (*m/z* (%)): 304 (68) [Me₄Sb₂]⁺, 289 (24) [Me₃Sb₂]⁺, 250 (21) [MeSbIn]⁺, 166 (7) [Me₃Sb]⁺, 151 (23) [Me₂Sb]⁺, 145, (100) [Me₂In]⁺, 136 (3) [MeSb]⁺.

[Me₂GaSb(*i*-Pr)₂]₃ (4; M_r = 923.15). A 2 mmol portion of Sb₂(*i*-Pr)₄ (2 mmol, 0.83 g) was added to a solution of 3.8 mmol of GaMe₃ (0.44 g) dissolved in 40 mL of pentane. The resulting yellow solution was stirred for 48 h at ambient temperature in the absence of light, yielding colorless solutions. The solvent was reduced to 5 mL and the solution stored at -30 °C. After 4 weeks, colorless crystals of **4** formed. Yield: 0.23 g, 0.25 mmol, 12% (based on the distibine). Mp: 84–89 °C dec. Anal. Found (calcd) for C₂₄H₆₀Ga₃Sb₃: C, 30.94 (31.24); H, 6.16 (6.61). ¹H NMR (300 MHz, C₆D₅H, 25 °C): δ 0.32 (s, 6 H, Me/Ga), 1.4 (d, ³J_{HH} = 7.8 Hz, 12 H, Me₂CH/Sb), 2.37 (sept, ³J_{HH} = 7.8 Hz, 2 H, Me₂CH/Sb). ¹³C{¹H} NMR (80 MHz, C₆D₅H, 25 °C): δ 14.4 (s, Me₂CH/Sb), 20.3 (s, b, Me₃C/Al), 24.9 (s, Me₂CH/Sb), 31.4 (Me₃C/Al). ¹³C{¹H} NMR (75 MHz, C₆D₆, 25 °C): δ 1.4 (s, Me/Ga), 24.9 (s, Me₂CH/Sb), 25.8 (s, Me₂CH/Sb).

(11) Lehmkuhl, H.; Olbrysch, O.; Nehl, H. *Liebigs Ann. Chem.* **1973**, 708.

(12) Coates, G. E.; Wade, K. In *Organometallic Compounds, The Main Group Elements*; Methuen: London, 1967.

(13) Reier, F. W.; Wolfram, P.; Schumann, H. *J. Cryst. Growth* **1988**, 93, 41.

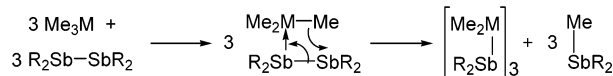
(14) Breunig, H. J.; Breunig-Lyriti, V.; Knobloch, T. P. *Chem. Z.* **1977**, 101, 399.

(15) Meinema, H. A.; Martens, H. F.; Noltes, J. G. *J. Organomet. Chem.* **1973**, 51, 223.

(16) Breunig, H. J.; Kanig, W. *J. Organomet. Chem.* **1980**, 186, C5.

(17) Breunig, H. J.; Müller, D. *Angew. Chem., Int. Ed. Engl.* **1982**, 21, 439.

Scheme 1



After filtration of **2–4** the solvent of each resulting solution was removed in vacuo. Oily residues were obtained, which were investigated by ¹H NMR. Resonances due to unconsumed MMe₃ (M = Ga (**2**, **4**), δ -0.15; M = In (**3**), δ -0.18) were observed. Additional resonances due to the formation of SbMe₃ (**2**, **3**, δ 0.60) were found, strongly supporting the proposed reaction mechanism (Scheme 1). The oily residue obtained from the synthesis of **4** showed several signals due to the presence of *i*-Pr (δ 1.20–1.37 (d, CHMe₂), 1.65–1.83 (sept, CHMe₂)) and Me groups (δ 0.54–0.62). To the best of our knowledge, *i*-Pr₂SbMe has not been identified by ¹H NMR, to date, allowing no comparison with these data. The presence of several resonances can be explained by ligand exchange reactions, leading to a mixture of several stibines of the type *i*-Pr_{3-x}SbMe_x (x = 0–3).

Preparation of Et₃Bi-M(*t*-Bu)₃. A 1 mmol portion of Bi₂Et₄ and 2 mmol of M(*t*-Bu)₃ (M = Al, Ga) were dissolved in 30 mL of pentane and stirred for 72 h at ambient temperature in the absence of light. The resulting black suspension was filtered and the light yellow filtrate was reduced to 5 mL and stored at -30 °C. After 48 h, **5** and **6** were obtained as colorless crystals.

Et₃Bi-Al(*t*-Bu)₃ (5; M_r = 494.50). Yield: 0.32 g, 0.65 mmol, 65%. Mp: 72–73 °C. Anal. Found (calcd) for C₁₈H₄₂AlBi: C, 42.86 (43.71); H, 8.11 (8.63). ¹H NMR (300 MHz, C₆D₅H, 25 °C): δ 1.13 (s, 27 H, Me₃C/Al), 1.65–1.76 (m, 15 H, Et/Bi). ¹³C{¹H} NMR (80 MHz, C₆D₅H, 25 °C): δ 10.4 (s, b, CH₃CH₂/Bi), 13.0 (s, CH₃CH₂/Bi), 20.7 (s, b, Me₃C/Al), 31.0 (s, Me₃C/Al).

Et₃Bi-Ga(*t*-Bu)₃ (6; M_r = 537.23). Yield: 0.21 g, 0.34 mmol, 39%. Mp: 46–48 °C. Anal. Found (calcd) for C₁₈H₄₂-GaBi: C, 39.78 (38.78); H, 7.11 (6.75). ¹H NMR (300 MHz, C₆D₅H, 25 °C): δ 1.20 (s, 27 H, Me₃C/Ga), 1.63–1.77 (m, 15 H, Et/Bi). ¹³C{¹H} NMR (80 MHz, C₆D₅H, 25 °C): δ = 10.3 (s, b, CH₃CH₂/Bi), 13.1 (s, CH₃CH₂/Bi), 22.6 (s, b, Me₃C/Ga), 31.4 (s, Me₃C/Ga).

X-ray Structure Solution and Refinement. Crystallographic data of **1–4** are summarized in Table 1 and those of **5** and **6** in Table 2. Selected bond lengths and angles are given in Table 3 (**2–4**) and Table 4 (**5** and **6**). Figures 1–6 show ORTEP diagrams of the solid-state structures of **1–6**. Data were collected on a Nonius Kappa-CCD diffractometer using Mo K α radiation (λ = 0.710 73 Å) at *T* = -150 °C, and the structures were solved by direct methods (**1–4**, **6**) and Patterson methods (SHELXS-97;¹⁸ respectively, and refined by full-matrix least-squares on *F*². Empirical absorption corrections were applied for all compounds. All non-hydrogen atoms in **1–6** were refined anisotropically, and hydrogen atoms were refined by a riding model (SHELXL-97).¹⁹

Results and Discussion

To establish the distibine cleavage reaction as a general reaction type for the formation of completely alkyl substituted heterocycles of the type [R₂MSbR'₂]_x (M = Al, Ga, In) and to verify the influence of the organic ligands bound to the metal centers on the formation of the M-Sb heterocycles, reactions of three distibines Sb₂R'₄ (R' = Me, Et, *i*-Pr) with AlR₃ (R = Me, Et, *t*-Bu), GaMe₃, and InMe₃ were investigated. Unfor-

(18) Sheldrick, G. M. SHELXS-97, Program for Structure Solution. *Acta Crystallogr., Sect. A* **1990**, 46, 467.

(19) Sheldrick, G. M. SHELXL-97, Program for Crystal Structure Refinement; Universität Göttingen, Göttingen, Germany, 1997.

Table 1. Crystallographic Data and Measurement Details for [*i*-Pr₄Sb₂][Al(*t*-Bu)₃]₃ (1), [Me₂GaSbMe₂]₃ (2), [Me₂InSbMe₂]₃ (3), [Me₂GaSb(*i*-Pr)₂]₃ (4)

	1	2	3	4
mol formula	C ₂₄ H ₅₅ AlSb ₂	C ₁₂ H ₃₆ Ga ₃ Sb ₃	C ₁₂ H ₃₆ In ₃ Sb ₃	C ₂₄ H ₆₀ Ga ₃ Sb ₃
fw	614.16	754.82	890.12	923.13
cryst syst	triclinic	triclinic	monoclinic	monoclinic
space group	$P\bar{1}$ (No. 2)	$P\bar{1}$ (No. 2)	$P2_1/n$ (No. 14)	$P2_1/c$ (No. 14)
<i>a</i> , Å	9.7698(5)	10.3280(3)	13.3859(3)	16.3795(2)
<i>b</i> , Å	10.2089(6)	10.4400(4)	10.6226(2)	10.4832(2)
<i>c</i> , Å	15.4554(9)	13.4815(6)	17.7192(4)	21.2972(3)
α, deg	78.255(3)	101.056(1)		
β, deg	78.374(3)	97.883(1)	100.684(1)	98.716(1)
γ, deg	89.431(3)	119.513(1)		
<i>V</i> , Å ³	1477.49(14)	1195.01(8)	2475.87(9)	3614.70(10)
<i>Z</i>	2	2	4	4
radiation (wavelength, Å)	Mo Kα (0.710 73)	Mo Kα (0.710 73)	Mo Kα (0.710 73)	Mo Kα (0.710 73)
μ, mm ⁻¹	1.865	6.664	5.963	4.423
temp. K	123(2)	123(2)	123	123(2)
<i>D</i> _{calcd} , g cm ⁻³	1.380	2.098	2.388	1.696
cryst dimens (mm)	0.15 × 0.10 × 0.10	0.20 × 0.15 × 0.15	0.20 × 0.10 × 0.05	0.50 × 0.30 × 0.25
2θ _{max} , deg	50	50	55	55
no. of rflns measd	12 969	10 162	13 172	20 662
no. of nonequiv rflns measd	4967	4165	5500	8002
<i>R</i> _{merge}	0.067	0.044	0.047	0.053
no. of params refined	244	163	163	271
<i>R</i> ₁ , ^a <i>wR</i> ₂ ^b	0.038, 0.067	0.046, 0.104	0.026, 0.064	0.027, 0.0608
goodness of fit ^c	0.899	1.064	1.021	0.992
final max, min Δρ, e Å ⁻³	0.993, -0.711	2.693, -1.603	0.994, -1.215	0.982, -1.186

^a *R*₁ = Σ(|*F*_o| - |*F*_c|)/Σ|*F*_o| (for *I* > 2σ(*I*)). ^b *wR*₂ = {Σ[*w*(*F*_o² - *F*_c²)²]/Σ[*w*(*F*_o²)²]}^{1/2}. ^c Goodness of fit = {Σ[*w*(*F*_o² - |*F*_c²)|]/(N_{observns} - N_{params})}^{1/2}.

Table 2. Crystallographic Data and Measurement Details for Et₃Bi-Al(*t*-Bu)₃ (5) and Et₃Bi-Ga(*t*-Bu)₃ (6)

	5	6
mol formula	C ₁₈ H ₄₂ AlBi	C ₁₈ H ₄₂ BiGa
fw	494.48	537.22
cryst syst	monoclinic	monoclinic
space group	$P2_1/c$ (No. 14)	$P2_1/c$ (No. 14)
<i>a</i> , Å	14.1961(2)	14.1630(2)
<i>b</i> , Å	9.6925(1)	9.7255(1)
<i>c</i> , Å	16.0793(2)	16.0724(2)
β, deg	91.0310(10)	90.848(1)
<i>V</i> , Å ³	2212.08(5)	2213.61(5)
<i>Z</i>	4	4
radiation (wavelength, Å)	Mo Kα (0.710 73)	Mo Kα (0.710 73)
μ, mm ⁻¹	8.004	9.149
temp. K	123(2)	123(2)
<i>D</i> _{calcd} , g cm ⁻³	1.485	1.612
crystal dim. (mm)	0.50 × 0.40 × 0.30	0.60 × 0.55 × 0.50
2θ _{max} , deg	50.0	50.0
no. of rflns measd	40 217	40 044
no. of nonequiv rflns measd	3881	3890
<i>R</i> _{merge}	0.058	0.077
no. of params refined	181	181
<i>R</i> ₁ , ^a <i>wR</i> ₂ ^b	0.018, 0.044	0.0249, 0.067
goodness of fit ^c	1.080	1.073
final max, min Δρ, e Å ⁻³	0.560, -1.154	1.748, -1.164

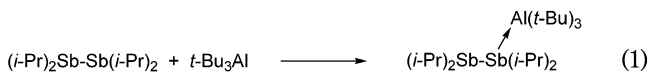
^a *R*₁ = Σ(|*F*_o| - |*F*_c|)/Σ|*F*_o| (for *I* > 2σ(*I*)). ^b *wR*₂ = {Σ[*w*(*F*_o² - *F*_c²)²]/Σ[*w*(*F*_o²)²]}^{1/2}. ^c Goodness of fit = {Σ[*w*(*F*_o² - |*F*_c²)|]/(N_{observns} - N_{params})}^{1/2}.

tunately, reactions with AlR₃ in pentane at ambient temperature occurred with decomposition of the distibine and formation of insoluble black residues which could not be identified. However, the Lewis acid–base adduct [*i*-Pr₄Sb₂][Al(*t*-Bu)₃]₃ (**1**) was isolated as a crystalline solid in moderate yield from the reaction of Sb₂(*i*-Pr)₄ with either 1 or 2 equiv of Al(*t*-Bu)₃ (eq 1). To

the best of our knowledge, **1** is the first mononuclear distibine complex to be structurally characterized to date.

The ¹H NMR spectrum of **1** showed resonances due to the organic ligands (*i*-Pr, *t*-Bu) in a 4:3 molar ratio, indicating the formation of a mononuclear adduct. Its mass spectrum only showed signals due to fragmentation reactions (Sb₂(*i*-Pr)₄ and Al(*t*-Bu)₃). Single crystals of **1** suitable for an X-ray structure determination were obtained from a solution in pentane at -60 °C. Figure 1 shows the solid-state structure of **1**.

1 crystallizes in the triclinic space group $P\bar{1}$ (No. 2). The Sb–Sb bond distance in **1** (2.855(1) Å) is comparable to those observed for dinuclear distibine adducts [R₄Sb₂][Al(*t*-Bu)₃]₂ (R = Me, 2.811(1) Å; R = Et, 2.838(1) Å) and the uncomplexed distibines (Sb₂Me₄, 2.862(2) Å²⁰ and 2.830(1), 2.838(1) Å;²¹ Sb₂(SiMe₃)₄, 2.867(1) Å;²² Sb₂(SnMe₃)₄, 2.866(1) Å;²³ Sb₂(*t*-Bu)₄, 2.817(1) Å;²⁴ Sb₂Ph₄, 2.844(1) Å²²). The Al–Sb bond length observed for **1** (3.003(2) Å) is elongated compared to those observed for [Me₄Sb₂][Al(*t*-Bu)₃]₂ (2.919(1) Å) and [Et₄Sb₂][Al(*t*-Bu)₃]₂ (3.001(1) Å), clearly reflecting the increased repulsive interactions between the organic substituents. The most interesting structural feature of **1** is displayed by the degree of pyramidalization observed at the central Sb atoms. The sum of the C–Sb–C and C–Sb–Sb bond angles found for the uncomplexed Sb center (Sb1, 300.9°) is significantly larger than that of the Sb atom which is coordinated to the alane (Sb2, 288.2°). It is also much larger than that observed for



(20) Ashe, A. J., III; Ludwig, E. G., Jr.; Oleksyszyn, J.; Huffman, J. C. *Organometallics* **1984**, *3*, 337.

(21) Mundt, O.; Riffel, H.; Becker, G.; Simon, A. *Z. Naturforsch.*, **1984**, *39*, 317.

(22) Becker, G.; Freudenblum, H.; Witthauer, C. *Z. Anorg. Allg. Chem.* **1982**, *492*, 37.

(23) Becker, G.; Meiser, M.; Mundt, O.; Weidlein, J. *Z. Anorg. Allg. Chem.* **1989**, *569*, 62.

(24) Mundt, O.; Becker, G.; Wessely, H.-J.; Breunig, H. J.; Kischkel, H. *Z. Anorg. Allg. Chem.* **1982**, *486*, 70.

Table 3. Selected Bond Lengths (Å) and Angles (deg) for 2–4

[Me ₂ GaSbMe ₂] ₃ (2)			
Sb1–Ga1	2.682(1)	Sb2–C6	2.134(8)
Sb1–Ga2	2.676(1)	Sb3–C9	2.147(8)
Sb2–Ga2	2.668(1)	Sb3–C10	2.160(9)
Sb2–Ga3	2.669(1)	Ga1–C3	1.983(9)
Sb3–Ga1	2.666(1)	Ga1–C4	1.983(9)
Sb3–Ga3	2.671(1)	Ga2–C7	2.000(10)
Sb1–C1	2.170(9)	Ga2–C8	2.003(9)
Sb1–C2	2.150(9)	Ga3–C11	1.989(8)
Sb2–C5	2.157(8)	Ga3–C12	1.979(9)
Ga1–Sb1–Ga2	130.8(1)	C1–Sb1–C2	99.0(4)
Ga1–Sb3–Ga3	136.7(1)	C5–Sb2–C6	98.2(4)
Ga2–Sb2–Ga3	129.7(1)	C10–Sb3–C9	97.2(4)
Sb1–Ga1–Sb3	97.3(1)	C3–Ga1–C4	118.2(4)
Sb1–Ga2–Sb2	107.8(1)	C7–Ga2–C8	119.3(5)
Sb2–Ga3–Sb3	98.5(1)	C11–Ga3–C12	117.7(4)
[Me ₂ InSbMe ₂] ₃ (3)			
Sb1–In1	2.845(1)	Sb2–C6	2.154(4)
Sb1–In3	2.852(1)	Sb3–C9	2.152(4)
Sb2–In1	2.842(1)	Sb3–C10	2.162(4)
Sb2–In2	2.869(1)	In1–C3	2.185(4)
Sb3–In2	2.858(1)	In1–C4	2.175(4)
Sb3–In3	2.844(1)	In2–C7	2.188(4)
Sb1–C1	2.150(5)	In2–C8	2.178(4)
Sb1–C2	2.143(4)	In3–C11	2.176(4)
Sb2–C5	2.151(4)	In3–C12	2.178(4)
In1–Sb1–In3	133.9(1)	C1–Sb1–C2	98.3(2)
In1–Sb2–In2	132.5(1)	C5–Sb2–C6	95.5(2)
In2–Sb3–In3	137.5(1)	C9–Sb3–C10	98.3(2)
Sb1–In1–Sb2	104.6(1)	C3–In1–C4	118.0(2)
Sb2–In2–Sb3	102.1(1)	C7–In2–C8	123.5(2)
Sb1–In3–Sb3	103.5(1)	C11–In3–C12	122.2(2)
[Me ₂ GaSb(<i>i</i> -Pr) ₂] ₃ (4)			
Sb1–Ga1	2.669(1)	Sb2–C12	2.182(3)
Sb1–Ga3	2.669(1)	Sb3–C17	2.177(3)
Sb2–Ga1	2.677(1)	Sb3–C20	2.174(3)
Sb2–Ga2	2.687(1)	Ga1–C7	1.994(4)
Sb3–Ga2	2.694(1)	Ga1–C8	1.972(4)
Sb3–Ga3	2.692(1)	Ga2–C15	1.985(3)
Sb1–C1	2.178(3)	Ga2–C16	1.973(3)
Sb1–C4	2.186(3)	Ga3–C23	1.983(3)
Sb2–C9	2.178(3)	Ga3–C24	1.990(3)
Ga1–Sb1–Ga3	118.9(1)	C1–Sb1–C4	102.0(1)
Ga1–Sb2–Ga2	127.7(1)	C9–Sb2–C12	97.4(1)
Ga2–Sb3–Ga3	130.5(1)	C17–Sb3–C20	97.8(1)
Sb1–Ga1–Sb2	104.1(1)	C7–Ga1–C8	119.8(2)
Sb1–Ga3–Sb3	102.2(1)	C15–Ga2–C16	117.5(2)
Sb2–Ga2–Sb3	103.7(1)	C23–Ga3–C24	118.6(2)

Table 4. Selected Bond Lengths (Å) and Angles (deg) for 5 and 6

Et ₃ Bi–Al(<i>t</i> -Bu) ₃ (5)			
Al1–Bi1	2.940(1)	Bi1–C13	2.249(3)
Al1–C1	2.019(3)	Bi1–C15	2.240(3)
Al1–C5	2.027(3)	Bi1–C17	2.249(3)
Al1–C9	2.017(3)		
C1–Al1–C5	116.9(1)	C13–Bi1–C15	96.2(2)
C1–Al1–C9	117.1(1)	C13–Bi1–C17	95.9(2)
C5–Al1–C9	117.5(1)	C15–Bi1–C17	96.2(2)
Et ₃ Bi–Ga(<i>t</i> -Bu) ₃ (6)			
Ga1–Bi1	2.966(1)	Bi1–C13	2.244(5)
Ga1–C1	2.025(4)	Bi1–C15	2.255(5)
Ga1–C5	2.038(4)	Bi1–C13	2.264(5)
Ga1–C9	2.048(5)		
C1–Ga1–C5	117.2(2)	C13–Bi1–C15	95.2(2)
C1–Ga1–C9	117.6(2)	C13–Bi1–C17	95.4(2)
C5–Ga1–C9	117.5(2)	C15–Bi1–C17	95.3(2)

Sb₂Me₄ (average 283.1°). These findings do not agree with the structural trends previously observed for

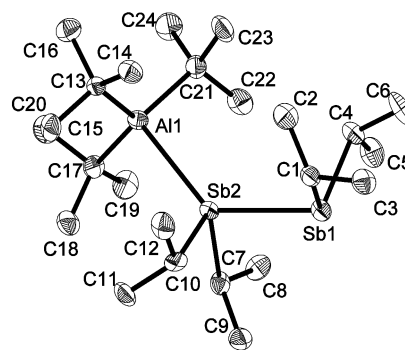


Figure 1. Ortep plot (ellipsoids at the 50% probability level; H atoms omitted for clarity) showing the solid-state structure and atom-numbering scheme for **1**. Selected bond lengths (Å) and angles (deg): Sb1–Sb2 = 2.855(1), Sb2–Al1 = 3.003(2), Al1–C13 = 2.024(5), Al1–C17 = 2.022(6), Al1–C21 = 2.040(5), Sb1–C1 = 2.191(5), Sb1–C4 = 2.208(5), Sb2–C7 = 2.179(5), Sb2–C10 = 2.204(5); C13–Al1–C17 = 116.0(2), C13–Al1–C21 = 115.0(2), C17–Al1–C21 = 116.4(2), C1–Sb1–C4 = 100.7(2), C1–Sb1–Sb2 = 97.5(2), C4–Sb1–Sb2 = 102.7(2), C7–Sb2–C10 = 96.3(2), C7–Sb2–Sb1 = 92.8(2), C10–Sb2–Sb1 = 99.1(2).

stibine²⁵ and distibine adducts,⁵ which typically show an increase of the sum of bond angles upon coordination to a Lewis acid due to an increase in p character of the former Sb electron lone pair and an increase in s character of the former Sb–C and Sb–Sb bonding electron pairs.²⁶ Obviously, repulsive interactions between the bulky *i*-Pr groups bound to the Sb center and the sterically demanding Lewis acid Al(*t*-Bu)₃ significantly influence the complex geometry. In addition, these repulsive steric interactions seem to prevent Sb₂(*i*-Pr)₄ from serving as a bidentate ligand, as was observed for Sb₂Me₄ and Sb₂Et₄. **1** shows Al–C bond distances (average 2.029 Å) and C–Al–C bond angles (average 115.8°) comparable to those of the dinuclear adducts [R₄Sb₂][Al(*t*-Bu)₃]₂ (R = Me, Et).⁵

Whereas the distibine cleavage reaction in our hands remained unsuccessful for the formation of Al–Sb heterocycles, reactions of Sb₂R₄ (R = Me, *i*-Pr) with 2 equiv of GaMe₃ and InMe₃ proceeded with cleavage of the Sb–Sb bond and subsequent formation of the corresponding six-membered Ga–Sb and In–Sb heterocycles [Me₂GaSbMe₂]₃ (**2**), [Me₂InSbMe₂]₃ (**3**), and [Me₂GaSb(*i*-Pr)₂]₃ (**4**) according to the mechanism described in Scheme 1.²⁷

However, the reactions described occurred much more slowly compared to those of Sb₂R₄ (R = Me, Et) with the sterically more demanding Lewis acid Ga(*t*-Bu)₃, which was found to react completely within 2 days.⁵ Solutions of Sb₂R₄ (R = Me, *i*-Pr) with 2 equiv of GaMe₃ and InMe₃ in pentane or toluene had to be stirred for 5–7 days at ambient temperature until a colorless solution was formed. Thereafter, the solvent was evacu-

(25) See the following and references therein: (a) Schulz, S.; Kuczkowski, A.; Nieger, M. *J. Organomet. Chem.* **2000**, *604*, 202. (b) Schulz, S.; Nieger, M. *J. Chem. Soc., Dalton Trans.* **2000**, 639.

(26) Unfortunately, the solid-state structure of Sb₂(*i*-Pr)₄ has not been determined, to date, allowing no structural comparisons between the sum of the bond angles of the uncomplexed distibine and **1**.

(27) Only 1 equiv of MMe₃ is formally necessary for the formation of the heterocycles. However, the reaction proceeds faster with 1.8–2 equiv of MMe₃, most likely due to the complexation of the trialkylstibine R₂SbMe (R = Me, Et, *i*-Pr) formed according to the reaction mechanism.

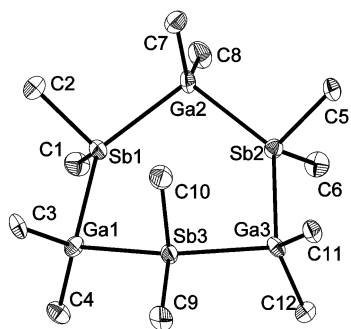


Figure 2. Ortep plot (ellipsoids at the 50% probability level; H atoms omitted for clarity) showing the solid-state structure and atom-numbering scheme for **2**.

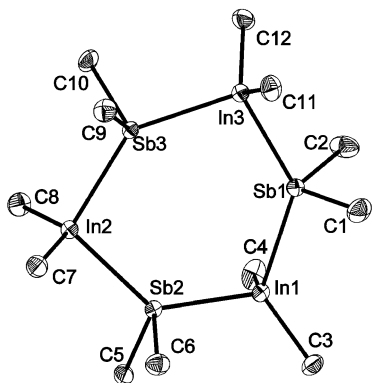
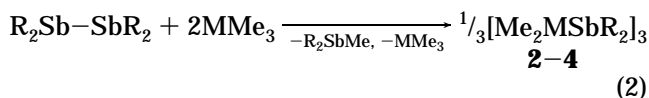


Figure 3. Ortep plot (ellipsoids at the 50% probability level; H atoms omitted for clarity) showing the solid state structure and atom-numbering scheme for **3**.

ated in vacuo, and the resulting waxy residues were dissolved in pentane (5 mL) and stored at $-60\text{ }^\circ\text{C}$. Colorless solids of **2–4** were formed within 3 days in moderate yields (eq 2).



M = Ga, R = Me (**2**), *i*-Pr (**4**); M = In, R = Me (**3**)

^1H and ^{13}C NMR spectra of **2–4** show signals due to the organic ligands in a 1:1 molar ratio, indicating the formation of the heterocycles. Mass spectra of **2–4** do not show molecular ion peaks due to fragmentation reactions. Single crystals of **2–4** suitable for X-ray diffraction were obtained from solutions in pentane at $-60\text{ }^\circ\text{C}$ (Figures 2–4).

2 crystallizes in the triclinic space group $P\bar{1}$ (No. 2), and **3** and **4** crystallize in the monoclinic space groups $P2_1/n$ (No. 14; **3**) and $P2_1/c$ (No. 14; **4**). The central structural motifs are the six-membered M–Sb rings, which adopt distorted-twist-boat conformations. The central group 13 metal and Sb atoms reside in distorted-tetrahedral environments. As was found previously, the ring size of the M–Sb heterocycles in the solid state depends on the steric bulk of the substituents bound to the metal centers, with the small Me groups favoring the formation of six-membered rings.²⁸ The Ga–Sb bond distances in **2** and **4** range from 2.668(1) to 2.694(1) Å. These distances are comparable to those found for other six-membered rings $[Me_2GaSb(SiMe_3)_2]_3$ (2.677(1)–2.714(1) Å),²⁹ $[Cl_2GaSb(t-Bu)_2]_3$ ³⁰ (2.659(1)–2.662(1) Å),

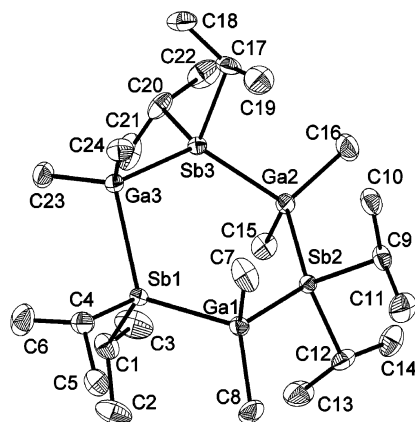


Figure 4. Ortep plot (ellipsoids at the 50% probability level; H atoms omitted for clarity) showing the solid-state structure and atom-numbering scheme for **4**.

and $[t\text{-Bu}_2GaSbMe_2]_3$ (2.713(1)–2.751(1) Å).⁵ The endocyclic Ga–Sb–Ga bond angles observed for **2** (129.7(1)–136.7(1) $^\circ$) are significantly increased compared to those observed for **4** (118.9(1)–130.5(1) $^\circ$), whereas the Ga–C bond distances of **2** and **4** (average values: 1.983 Å, **2**; 1.985 Å, **4**) are almost the same. In contrast, the average Sb–C bond length observed for **2** (2.153 Å) is significantly shorter than that of **4** (2.179 Å), clearly demonstrating the influence of the larger *i*-Pr substituents.

The In–Sb bond distances in **3** range from 2.842(1) to 2.869(1) Å, which are comparable to those previously reported for six-membered stibinoindanes $[Me_2InSb(SiMe_3)_2]_3$ (2.844(1)–2.870(1) Å),²⁸ $[Et_2InSb(SiMe_3)_2]_3$ (2.824(2)–2.911(2) Å),³¹ and $[Me_2InSb(CH_2SiMe_3)_2]_3$ (2.852(2)–2.869(2) Å).⁷ In contrast, those observed for the four-membered heterocycle $[t\text{-Bu}_2InSb(SiMe_3)_2]_2$ are significantly longer (2.927(1)–2.934(2) Å) due to increased repulsive interactions between the larger organic substituents.³² As was observed for the Ga–Sb heterocycles **2** and **4**, the endocyclic In–Sb–In bond angles of **3** (132.5(1)–137.5(1) $^\circ$) are larger than the Sb–In–Sb angles (102.1(1)–104.6(1) $^\circ$). The In–C bond distances (average value 2.179 Å) and Sb–C bond lengths (average value 2.152 Å) are within the expected ranges.

Since the distibine cleavage reaction gives an easy access to completely alkyl substituted, heterocyclic stibinogallanes and -indanes, we became interested in whether this reaction pathway also allows the generation of group 13–Bi heterocycles of the general type $[R_2MBiR'_2]_x$ (M = Al, Ga). To date, only three compounds of the desired type have been prepared by dehydrosilylation reactions between $Bi(SiMe_3)_3$ and Me_2MH (M = Al,³³ Ga³⁴) as well as by a novel meta-

(28) For a detailed structural comparison of M–Sb heterocycles see: Thomas, F.; Schulz, S.; Nieger, M. *Z. Anorg. Allg. Chem.* **2002**, *628*, 235.

(29) Schulz, S.; Nieger, M. *J. Organomet. Chem.* **1998**, *570*, 275.

(30) Cowley, A. H.; Jones, R. A.; Kidd, K. B.; Nunn, C. M.; Westmoreland, D. L. *J. Organomet. Chem.* **1988**, *341*, C1.

(31) Foos, E. E.; Jouet, R. J.; Wells, R. L.; White, P. S. *J. Organomet. Chem.* **2000**, *598*, 182.

(32) Foos, E. E.; Wells, R. L.; Rheingold, A. L. *J. Cluster Sci.* **1999**, *10*, 121.

(33) Schulz, S.; Nieger, M. *Angew. Chem., Int. Ed. Engl.* **1999**, *38*, 967.

(34) Thomas, F.; Schulz, S.; Nieger, M. *Organometallics* **2002**, *21*, 2793.

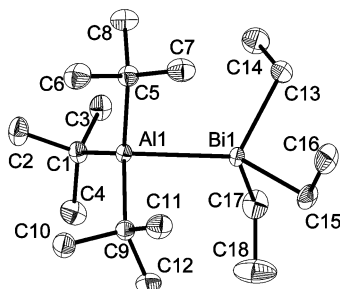


Figure 5. Ortep plot (ellipsoids at the 50% probability level; H atoms omitted for clarity) showing the solid-state structure and atom-numbering scheme for **5**.

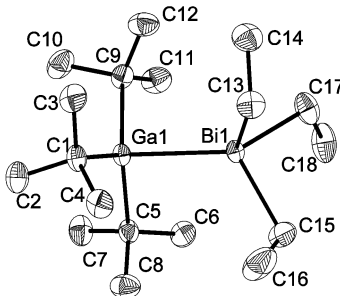
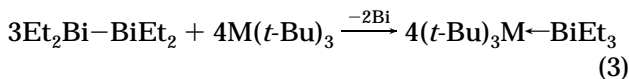


Figure 6. Ortep plot (ellipsoids at the 50% probability level; H atoms omitted for clarity) showing the solid-state structure and atom-numbering scheme for **6**.

thesis reaction between $[\text{Me}_2\text{AlBi}(\text{SiMe}_3)_2]_3$ and dmap-InMe_3 .³⁵ Since the stability of the E–E bond of dipentetes $\text{E}_2\text{R}'_4$ steadily decreases with increasing atomic number of the group 15 element, dibismuthines $\text{Bi}_2\text{R}'_4$ are even less stable than distibines $\text{Sb}_2\text{R}'_4$. Consequently, complexes of dibismuthines remained unknown until we reported only recently on the synthesis and single-crystal X-ray structures of the first stable dinuclear dibismuthine–alane and –gallane adducts $[\text{Et}_4\text{Bi}_2][\text{M}(\text{t-Bu})_3]_2$ (M = Al, Ga).⁶ However, the lability of the Bi–Bi bond renders dibismuthines very interesting starting compounds for further reactions, and we now report on the reaction of Bi_2Et_4 with $\text{M}(\text{t-Bu})_3$.

Bi_2Et_4 was reacted with 1 or 2 equiv of $\text{M}(\text{t-Bu})_3$ in pentane, toluene, or THF in the temperature range from -30 to 25 °C, resulting in the formation of black residues. Filtration of the insoluble material yielded light yellow filtrates, which were stored at -60 °C. Colorless crystals of $\text{Et}_3\text{Bi-M}(\text{t-Bu})_3$ (M = Al (**5**), Ga (**6**)) were formed within 48 h (eq 3).



^1H and ^{13}C NMR spectra of **5** and **6** show resonances due to the Et and *t*-Bu groups in a 1:1 molar ratio. Peaks with the highest mass found in the mass spectra of **5** and **6** correspond to $[\text{M}(\text{t-Bu})_3]^+$ (m/z 198, **5**; m/z 240, **6**) and $[\text{BiEt}_3]^+$ (m/z 296). The solid-state structures of **5** and **6** were determined by single-crystal X-ray diffraction. Figures 5 and 6 show the solid-state structures of **5** and **6**.

5 and **6** are isostructural and crystallize in the monoclinic space group $P2_1/c$ (No. 14). The central metal atoms reside in distorted-tetrahedral environments with their substituents adopting a staggered conformation relative to one another, as is typical for such adducts.

The central M–Bi bond distances are significantly elongated (2.940(1) Å, **5**; 2.966(1) Å, **6**) compared to the sum of the covalent radii (2.75 Å (AlBi), 2.76 Å (GaBi))³⁶. They are comparable to those found for $\text{Et}_3\text{M-Bi}(\text{SiMe}_3)_3$ adducts (M = Al, 2.921(2) Å; M = Ga, 2.966(1) Å) but significantly shorter than those reported for the sterically more hindered bismuthine and dibismuthine adducts of the type $(\text{t-Bu})_3\text{M-Bi}(\text{i-Pr})_3$ (M = Al, 3.088(1) Å; M = Ga, 3.135(1) Å)³⁷ and $[\text{Et}_4\text{Bi}_2][\text{M}(\text{t-Bu})_3]_2$ (M = Al, 3.084(1) Å; M = Ga, 3.099(2) and 3.114(2) Å)⁶. The sum of the C–M–C bond angles of the $\text{M}(\text{t-Bu})_3$ units (351.5°, **5**; 352.3°, **6**), which deviate only by 8° from planarity, indicate only weak Lewis acid–base interactions, as was previously observed for the bismuthine and dibismuthine adducts. The M–C (average values: 2.011 Å, **5**; 2.037 Å, **6**) and Bi–C bond lengths (average values: 2.246 Å, **5**; 2.254 Å, **6**) are within typical ranges.

The formation of **5** and **6** clearly shows the strong tendency of Bi_2Et_4 to disproportionate with formation of elemental Bi and BiEt_3 .¹⁷ This trend, which has also been observed for Bi_2Ph_4 ,³⁸ is typical for dibismuthines. BiEt_3 reacts with the Lewis acid $\text{M}(\text{t-Bu})_3$ with formation of the corresponding adducts.

Summary. Reactions of distibines $\text{Sb}_2\text{R}'_4$ with trialkylalanes, -gallanes, and -indanes MR_3 were investigated in detail, clearly demonstrating the distibine cleavage reaction to be a powerful reaction pathway for the synthesis of Ga–Sb and In–Sb heterocycles $[\text{R}_2\text{MSbR}'_2]_x$, whereas the corresponding Al–Sb heterocycles $[\text{R}_2\text{AlSbR}'_2]_x$ could not be obtained. However, for the first time the mononuclear distibine complex $[\text{i-Pr}_4\text{Sb}_2][\text{Al}(\text{t-Bu})_3]$ was synthesized and structurally characterized. The organic substituents R bound to the group 13 metal center were found to play a key role in the distibine cleavage reaction. Distibines $\text{Sb}_2\text{R}'_4$ (R = Me, Et) readily react with $\text{Ga}(\text{t-Bu})_3$, whereas reactions with GaMe_3 occur much more slowly and give the corresponding heterocycles in lower yields. These findings correlate with the Ga–C bond energy decreasing as the branching of the organic substituent increases.³⁹ In addition, the reactivity of the distibines $\text{Sb}_2\text{R}'_4$ toward ring formation was found to decrease with increasing steric demand of their substituents R', most likely due to their increased stability (principle of kinetic stabilization). Consequently, Sb_2Me_4 was found to be more reactive than $\text{Sb}_2(\text{i-Pr})_4$.

Reactions of Bi_2Et_4 with $\text{M}(\text{t-Bu})_3$ (M = Al, Ga) did not occur with formation of the corresponding M–Bi heterocycles $[\text{t-Bu}_2\text{MBiEt}_2]_x$ but with disproportionation yielding elemental Bi and BiEt_3 . BiEt_3 reacts with $\text{M}(\text{t-Bu})_3$ to give the corresponding Lewis acid–base adducts $\text{Et}_3\text{Bi-M}(\text{t-Bu})_3$ (M = Al, Ga).

Acknowledgment. This work was financially supported by the Deutsche Forschungsgemeinschaft (DFG), Fonds der Chemischen Industrie (FCI), the Bundesmin-

(35) Thomas, F.; Schulz, S.; Mansikkamäki, H.; Nieger, M. *Angew. Chem., Int. Ed.* **2003**, *42*, 5641.

(36) Holleman, A. F.; Wiberg, E. *Lehrbuch der Anorganischen Chemie*, 101st ed.; Walter de Gruyter: Berlin, 1995; p 1838 ff.

(37) (a) Kuczkowski, A.; Schulz, S.; Nieger, M. *Eur. J. Inorg. Chem.* **2001**, 2605. (b) Kuczkowski, A.; Thomas, F.; Schulz, S.; Nieger, M. *Organometallics* **2000**, *19*, 5758.

(38) Wiberg, E.; Mödritzer, K. *Z. Naturforsch., B* **1957**, *12*, 132.

(39) Ga–C bond energies: GaMe_3 , 264 kJ/mol; GaEt_3 , 209 kJ/mol. McMillen, D. F.; Golden, D. M. *Annu. Rev. Phys. Chem.* **1982**, *33*, 493.

isterium für Bildung, Wissenschaft, Forschung und Technologie (BMBF) and Prof. E. Niecke.

Supporting Information Available: Tables of bond distances, bond angles, anisotropic temperature factor param-

eters, and fractional coordinates for **1–6**; these data are also available in CIF format. This material is available free of charge via the Internet at <http://pubs.acs.org>.

OM049746M